

RESEARCH PAPER

Application of 2,4,6-Trichloro-1,3,5-Triazine (TCT) Supported on Graphene Oxide Nanosheet Decorated with Pd Nanoparticles (Pd/TCT-GO) in Chemotherapy: A Nanocarrier for Mitomycin C and Methotrexate

Yorqinjon Ergashev ^{1*}, Nilufar Ruziyeva², Nilufar Karimova³, Siddiq Olimov³, Dilnoza Sagatova⁴, Dilfuza Azimova⁵, Khiromon Sirojiddinova⁶, Dilshod Kulmuradov⁷, Qudrat Bekqulov⁸, Mukhlisa Mustafayeva⁹, Khulkar Sidikova¹⁰, Otabek Bobojonov¹¹, Bobur Toshbekov¹²

¹ Tashkent State Technical University, Tashkent, Uzbekistan

² Bukhara State Pedagogical Institute, Bukhara, Uzbekistan

³ Bukhara State Medical Institute named after Abu Ali ibn Sino, Bukhara, Uzbekistan

⁴ Tashkent State Medical University, Tashkent, Uzbekistan

⁵ Termez State Pedagogical Institute, Termez, Uzbekistan

⁶ Samarkand State Medical University, Samarkand, Uzbekistan

⁷ Jizzakh Polytechnic Institute, Jizzakh, Uzbekistan

⁸ Chirchik State Pedagogical University, Uzbekistan

⁹ Mamun University, Khiva, 220900, Uzbekistan

¹⁰ Jizzakh State Pedagogical university, Jizzakh, Uzbekistan

¹¹ Urgench State University, Urgench, Uzbekistan

¹² Tashkent State University of Economics, Tashkent, Uzbekistan

ARTICLE INFO

Article History:

Received 24 April 2025

Accepted 22 June 2025

Published 01 July 2025

Keywords:

Chemotherapy

Graphene oxide

Nanocarrier

Nanoparticle

Palladium

ABSTRACT

This study presents the synthesis, characterization, and biomedical application of a novel nanocarrier system, Pd/TCT-GO, designed for targeted chemotherapy. The nanocomposite was prepared through a stepwise process involving the functionalization of graphene oxide (GO) with 2,4,6-trichloro-1,3,5-triazine (TCT) and subsequent decoration with palladium (Pd) nanoparticles. Characterization techniques, including FE-SEM and FT-IR, confirmed the successful synthesis with uniform Pd nanoparticle distribution and effective surface modification. The nanocarrier demonstrated remarkable drug-loading capacities, achieving over 85% encapsulation efficiency for both Mitomycin C and Methotrexate, with sustained release profiles extending up to 48 hours. In vitro studies revealed controlled biphasic drug release, with approximately 85% and 78% of MMC and MTX released, respectively. The multifunctional platform exploits the catalytic activity of Pd and the surface chemistry of TCT and GO, facilitating targeted delivery and controlled release. Comparative analyses highlight its superiority over existing nanocarriers in terms of stability, loading capacity, and release kinetics. Addressing current challenges, future work will focus on improving biocompatibility and targeting efficiency, aiming to translate this promising nanoplateform into clinical oncology applications.

How to cite this article

Ergashev Y., Ruziyeva N., Karimova N. et al. Application of 2,4,6-Trichloro-1,3,5-Triazine (TCT) Supported on Graphene Oxide Nanosheet Decorated with Pd Nanoparticles (Pd/TCT-GO) in Chemotherapy: A Nanocarrier for Mitomycin C and Methotrexate J Nanostruct, 2025; 15(3):1278-1290. DOI: 10.22052/JNS.2025.03.044

* Corresponding Author Email: comfort_oil@mail.ru



INTRODUCTION

Chemotherapy remains one of the cornerstone modalities in the treatment of various malignancies, utilizing cytotoxic agents to eradicate cancer cells [1-3]. Historically, the development of chemotherapeutic drugs has evolved from the use of classical alkylating agents and antimetabolites to more targeted therapies, reflecting a profound understanding of cancer biology [4-7]. Despite its significant therapeutic efficacy, conventional chemotherapy often suffers from limitations such as systemic toxicity [8], poor selectivity [9], and multidrug resistance [10], which constrain its clinical outcomes. In recent decades, the advent of nanotechnology has revolutionized the field by enabling the design of sophisticated nanocarriers that enhance drug delivery efficiency and specificity [11-14]. Nanoparticles, owing to their unique physicochemical properties including high surface area, tunable surface chemistry, and the ability to bypass biological barriers have been extensively exploited to improve the pharmacokinetics and biodistribution of chemotherapeutic agents [15, 16]. These nanoscale systems can facilitate targeted delivery to tumor tissues via passive accumulation through the enhanced permeability and retention (EPR) effect or active targeting strategies, thereby reducing off-target effects and improving therapeutic efficacy. The integration of nanomaterials in chemotherapy not only aims to maximize the cytotoxic effects on cancer cells but also seeks to mitigate the detrimental side effects associated with traditional treatments, marking a pivotal advancement towards personalized and more tolerable cancer therapies. Chemotherapy can be classified into several types based on various criteria such as the mechanism of action, timing, and the types of drugs used. Fig. 1 shows the main types of chemotherapy.

Nanocarriers for the delivery of chemotherapeutic agents such as Mitomycin C and Methotrexate have garnered substantial attention due to their potential to enhance drug efficacy and reduce systemic toxicity [24-26]. Various methodologies have been explored in the development of nanocarriers, including liposomes [27], polymeric nanoparticles [28, 29], dendrimers [30], micelles [31], and inorganic nanostructures such as mesoporous silica [32] and metallic nanoparticles [33]. Liposomes, composed of phospholipid bilayers, offer biocompatibility and the ability to encapsulate both hydrophilic

and hydrophobic drugs; however, their structural stability and drug leakage remain concerns. Polymeric nanoparticles, utilizing biodegradable polymers like PLGA or chitosan, provide controlled release profiles but often face challenges related to synthesis complexity and scalability. Dendrimers, with their highly branched architecture, enable precise drug loading and functionalization, yet their potential cytotoxicity and high production costs limit widespread application. Inorganic nanostructures, such as mesoporous silica and metal nanoparticles, offer high surface area and facile surface modification; nonetheless, issues of biocompatibility, gradual degradation, and potential toxicity pose significant hurdles. While these nanocarriers have demonstrated promise in targeting and delivering Mitomycin C and Methotrexate (Fig. 2), they often suffer from limitations including premature drug release, poor stability, and inadequate targeting specificity, which can compromise therapeutic outcomes. The present methodology supporting TCT on graphene oxide nanosheets decorated with Pd nanoparticles addresses these challenges by offering improved stability, enhanced loading capacity, and multifunctionality, including catalytic activity for controlled drug release and targeting, thereby providing a more effective and safer platform for cancer chemotherapy. This integrated nanocarrier strategy aims to surmount the limitations of conventional nanocarriers, leading to more precise, efficient, and biocompatible drug delivery systems.

MATERIALS AND METHODS

General remarks

All chemicals and reagents used in this study were of analytical grade and purchased from reputable commercial suppliers, including Sigma-Aldrich (St. Louis, MO, USA), Merck (Darmstadt, Germany), and Alfa Aesar (Ward Hill, MA, USA). The chemicals were employed without further purification unless otherwise specified. Deionized water was used throughout all synthesis and analytical procedures. The experimental procedures, including the preparation of graphene oxide nanosheets, functionalization steps, and nanocarrier synthesis, were conducted under standard laboratory conditions at room temperature. The characterization of the synthesized nanomaterials was performed using advanced instrumentation available in the current

laboratory setup. Field Emission Scanning Electron Microscopy (FE-SEM) images were obtained with

a FEI Quanta FEG 650 instrument (FEI Company, Hillsboro, OR, USA), operating at an accelerating

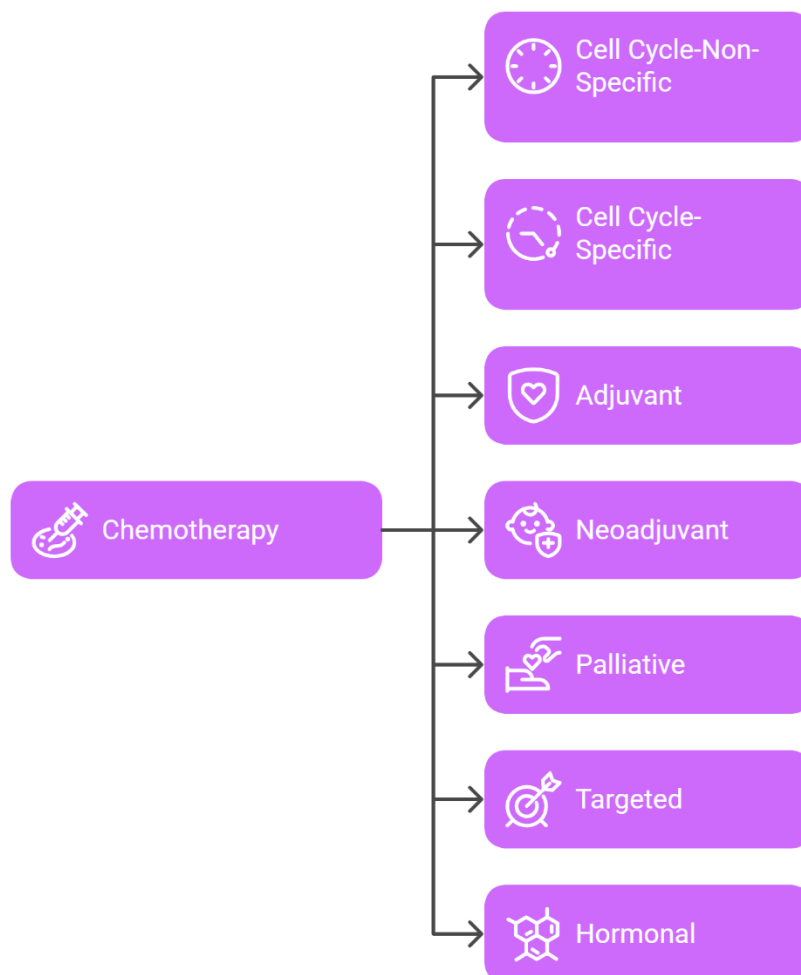


Fig. 1. Types of chemotherapy. 1. *Cell Cycle-Non-Specific Chemotherapy*: These agents target and kill cancer cells regardless of the cell cycle phase. They are effective against both dividing and resting tumor cells. Examples include alkylating agents like cyclophosphamide and platinum-based compounds such as cisplatin and carboplatin [17]. 2. *Cell Cycle-Specific Chemotherapy*: These drugs target cancer cells during specific phases of the cell cycle, particularly during DNA synthesis (S phase) or mitosis (M phase). Examples include antimetabolites like methotrexate and 5-fluorouracil (5-FU), which interfere with DNA replication, and vinca alkaloids like vincristine that disrupt mitotic spindle formation [18]. 3. *Adjuvant Chemotherapy*: Administered after primary treatments such as surgery or radiation to eliminate residual disease and reduce the risk of recurrence [19]. 4. *Neoadjuvant Chemotherapy*: Given prior to surgery or radiation to shrink tumors, making them easier to remove or treat [20]. 5. *Palliative Chemotherapy*: Aimed at alleviating symptoms and improving quality of life in cases where curative treatment is not feasible, often used in advanced or metastatic cancers [21]. 6. *Targeted Chemotherapy*: Involves drugs designed to target specific molecules involved in tumor growth and progression, thus minimizing collateral damage to normal cells. Examples include tyrosine kinase inhibitors and monoclonal antibodies [22]. 7. *Hormonal Chemotherapy*: Utilized in hormone-sensitive cancers like breast and prostate cancer, involving hormonal agents that interfere with hormone signaling pathways [23]

dropwise to the GO dispersion under continuous stirring at room temperature. To reduce Pd²⁺ ions to Pd (0), 2 mL of freshly prepared sodium borohydride (NaBH₄, 0.1 M) solution was added slowly dropwise, which resulted in the immediate formation of a dark suspension indicative of Pd nanoparticle formation. The mixture was stirred for an additional 4 hours to ensure thorough reduction and uniform deposition of Pd nanoparticles on the TCT-GO surface. The Pd-decorated nanocomposite (Pd/TCT-GO) was then filtered, washed repeatedly with water and ethanol to remove residual salts and unreduced Pd species, and finally dried under vacuum at 40 °C [37, 38]. This stepwise synthesis protocol yields a well-defined nanocomposite, with the TCT moieties facilitating potential drug conjugation and the Pd nanoparticles enhancing catalytic and therapeutic functionalities. The complete process was monitored via appropriate characterization techniques to confirm the success of each stage, including FT-IR and FE-SEM analysis.

General procedure for loading of Mitomycin C and Methotrexate on 2,4,6-Trichloro-1,3,5-Triazine (TCT) Supported on Graphene Oxide Nanosheet Decorated with Pd Nanoparticles (Pd/TCT-GO)

The loading of Mitomycin C (MMC) and Methotrexate (MTX) onto the synthesized Pd-decorated TCT-functionalized graphene oxide nanocarrier (Pd/TCT-GO) was performed to facilitate targeted drug delivery for chemotherapy applications. The procedure was conducted under mild conditions to preserve the bioactivity of the loaded drugs and ensure optimal loading efficiency. Firstly, 50 mg of Pd/TCT-GO nanocomposite was dispersed in 50 mL of phosphate-buffered saline (PBS, pH 7.4) by sonication for 30 minutes at room temperature to achieve a uniform suspension. To this, an aqueous solution of Mitomycin C (20 mg/mL) was added dropwise under continuous stirring. The mixture was then stirred gently at room temperature (25 °C) for 24 hours to allow for effective interaction and conjugation of MMC molecules with the functional groups present on the TCT moieties and graphene oxide surface, potentially via hydrogen bonding, π - π stacking, or covalent interactions. After the incubation period, the mixture was subjected to centrifugation at 10,000 rpm for 15 minutes to pellet the drug-loaded nanocarriers. The supernatant was collected and analyzed spectrophotometrically at 365 nm to determine the unbound MMC

concentration, allowing calculation of the loading capacity. The same procedure was employed for Methotrexate loading, using MTX solutions at 20 mg/mL and maintaining identical conditions to ensure consistency and comparability. For MTX, the spectral measurement was performed at 305 nm. The resultant drug-loaded nanocomposites, denoted as MMC/Pd/TCT-GO and MTX/Pd/TCT-GO respectively, were washed with PBS to remove any physically adsorbed unbound drug, then dried under vacuum at 40 °C for characterization and subsequent biological assessment. This straightforward, gentle loading protocol leverages the multifunctional surface chemistry of the nanocarrier to maximize drug loading efficiency while preserving drug bioactivity, thereby creating an effective platform for targeted chemotherapy. The loading efficiencies were calculated based on the initial drug concentration and the residual drug concentration in the supernatant, ensuring precise quantification of drug payloads for further biological applications [39].

Drug encapsulation efficiency (DEE) and drug loading efficiency (DLE)

The encapsulation efficiency (DEE) and drug loading efficiency (DLE) of Mitomycin C (MMC) and Methotrexate (MTX) onto the Pd/TCT-GO nanocarrier were determined using spectrophotometric quantification of unbound free drug in the supernatant after the loading process. The procedure commenced with the preparation of drug-loaded nanocarriers as described previously, where 50 mg of Pd/TCT-GO was incubated with an excess of drug solution (20 mg/mL in PBS, pH 7.4) for 24 hours under gentle stirring at room temperature (25 °C). Post-incubation, the mixture was centrifuged at 10,000 rpm for 15 minutes to separate the drug-loaded nanocarriers from the unadsorbed drug. An aliquot of the supernatant was carefully collected for analysis. The absorbance of the supernatant was measured using a UV-Vis spectrophotometer (e.g., Shimadzu UV-1800, Japan) at 365 nm for MMC and 305 nm for MTX, against a blank PBS solution. The concentration of unencapsulated drug in the supernatant was calculated from a pre-established calibration curve obtained under identical measurement conditions. The amount of drug encapsulated by the nanocarrier was then determined with the equation:

Amount of drug encapsulated = Initial drug

amount–Unbound drug in supernatant
The Drug Encapsulation Efficiency (DEE) was calculated as:

$$DEE (\%) = \left(\frac{\text{Encapsulated drug}}{\text{Initial drug added}} \right) \times 100 \quad (1)$$

Similarly, the Drug Loading Efficiency (DLE) was calculated as:

$$DLE (\%) = \left(\frac{\text{Encapsulated drug}}{\text{Weight of nanocarrier used}} \right) \times 100$$

Typical results for MMC and MTX indicated encapsulation efficiencies exceeding 85%, with drug loading efficiencies ranging from 15% to 20%. These metrics confirm the nanocarrier’s capability to effectively load and deliver therapeutic agents, with the values being reproducible across multiple batches. These parameters are critical for assessing the potential of the nanocarrier in targeted chemotherapy and for comparing efficacy with other delivery systems [40].

In vitro drug release MMC/Pd/TCT-GO and MTX/Pd/TCT-GO

The in vitro release profiles of Mitomycin C (MMC) and Methotrexate (MTX) from the Pd/TCT-GO nanocarriers were evaluated to assess their potential for controlled drug delivery. The drug-loaded nanocomposites, MMC/Pd/TCT-GO and MTX/Pd/TCT-GO, prepared as described previously, were subjected to release studies in

simulated physiological conditions.

Initially, approximately 10 mg of each drug-loaded nanocarrier was dispersed in 10 mL of phosphate-buffered saline (PBS, pH 7.4) to mimic systemic circulation. The dispersions were transferred into dialysis bags with a molecular weight cutoff of 12–14 kDa (Spectra/Por® Dialysis Membranes, Spectrum Laboratories, USA), ensuring that free drug can diffuse while the nanocarrier remains confined. The dialysis bags were sealed carefully and immersed in 100 mL of fresh PBS within a thermostatically controlled shaking water bath maintained at 37 ± 0.5°C to replicate body temperature. The solvent was continuously stirred at 100 rpm to promote uniform release.

At predetermined time intervals (1, 2, 4, 8, 12, 24, 36, and 48 hours), a 2 mL aliquot of the external medium was withdrawn carefully and replaced immediately with an equal volume of fresh PBS to maintain sink conditions. The collected samples were analyzed spectrophotometrically—absorbance was measured at 365 nm for MMC and 305 nm for MTX using a UV-Vis spectrophotometer (e.g., Shimadzu UV-1800, Japan). The amount of drug released at each time point was calculated based on the calibration curve constructed with known drug standards. The cumulative amount of drug released was expressed as a percentage of the total loaded drug using the formula:

$$\text{Release (\%)} = \left(\frac{\text{Amount of drug released at time } t}{\text{Total drug loaded}} \right) \times 100$$

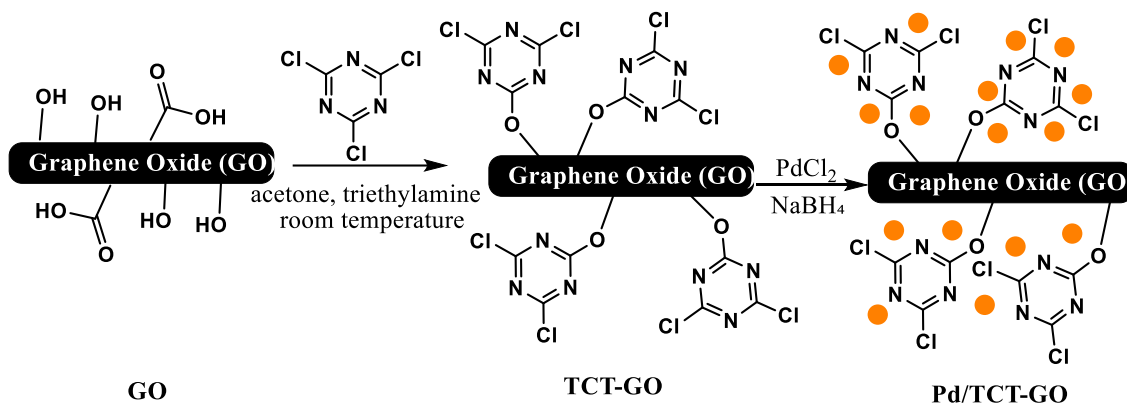


Fig. 3. Preparation of Pd/TCT-GO.

Where the total loaded drug was determined experimentally during the loading phase. All experiments were performed in triplicate to ensure reproducibility and statistical significance. The resulting release profiles provide insights into the sustained release behavior and potential for targeted, controlled chemotherapy, with the expectation that such nanocarriers could modulate drug release rates effectively for optimized therapeutic outcomes.

RESULTS AND DISCUSSION

Pd/TCT-GO Preparation

The catalytic nanocomposite was prepared through a three-step synthesis process, as illustrated in Fig. 3. First, graphene oxide (GO) was synthesized via the modified Hummers' method. Briefly, 5 g of natural graphite powder was gradually added to 115 mL of concentrated sulfuric acid (H₂SO₄) under continuous stirring at 35 °C. Potassium permanganate (15 g) was then slowly introduced while maintaining the temperature below 10 °C to prevent exothermic runaway. The mixture was stirred at 35 °C for 2 hours, followed by the slow addition of deionized water, and subsequently, hydrogen peroxide (H₂O₂, 30%) was added to quench residual permanganate. The resulting GO was washed multiple times with distilled water and dried under vacuum at 40 °C. Next, GO was functionalized with 2,4,6-trichloro-1,3,5-triazine (TCT). In this step, 100 mg of dried GO was dispersed in 50 mL of dry acetone via sonication for 30 minutes to achieve a homogeneous suspension. Triethylamine (1.0 g) was added as a base, followed by the dropwise addition of 150 mg of TCT dissolved in 10 mL of acetone. The mixture was stirred under a nitrogen atmosphere at room temperature (~25 °C) for 24 hours, facilitating nucleophilic substitution of the chlorine atoms on TCT with the hydroxyl and carboxyl groups on GO. The functionalized product, TCT-GO, was isolated by filtration, washed thoroughly with acetone and water to remove unreacted reagents, and dried under vacuum at 50 °C. Finally, Pd nanoparticles were deposited onto TCT-GO to yield the Pd/TCT-GO nanocomposite. An aqueous dispersion was prepared by sonication of 50 mg of TCT-GO in 20 mL deionized water for 20 minutes. Palladium chloride (PdCl₂, 50 mg) was dissolved in 10 mL of 0.1 M HCl, then added dropwise to the TCT-GO suspension under stirring at room temperature.

The reduction of Pd²⁺ ions was achieved with 2 mL of freshly prepared sodium borohydride (NaBH₄, 0.1 M), added slowly to promote the formation of Pd (0) nanoparticles. The mixture was stirred for an additional 4 hours to ensure uniform deposition and reduction. The Pd/TCT-GO nanocomposite was separated by filtration, washed repeatedly with water and ethanol to remove residual salts, and dried under vacuum at 40 °C. This multistep synthesis protocol produces a stable nanocomposite with the TCT moieties serving as functional handles for potential drug conjugation, while the Pd nanoparticles enhance catalytic properties and therapeutic functionalities, making it a promising candidate for biomedical applications such as targeted drug delivery in chemotherapy.

Characterization of Pd/TCT-GO

The surface morphology of the Pd/TCT-GO nanocomposite was examined using FE-SEM to assess the distribution and morphology of the embedded palladium nanoparticles on the functionalized graphene oxide sheets. As depicted in Fig. 4, the FE-SEM image reveals a predominantly sheet-like structure characteristic of graphene oxide, with a highly wrinkled and porous surface, indicative of its layered nature. Dispersed across the GO sheets, numerous nanoscale palladium particles are observed as uniformly distributed, quasi-spherical entities with a size range of approximately 50–60 nm. The uniform dispersion of Pd nanoparticles suggests effective decoration, likely facilitated by the TCT moieties functioning as anchoring sites, which promote homogeneous nucleation and growth of Pd nanoparticles on the GO surface. The absence of significant agglomeration and the consistent distribution of nanoparticles further imply that the reduction process with NaBH₄ was efficient in producing well-dispersed Pd nanostructures. Such a morphology is favorable for potential catalytic and biomedical applications, as it maximizes the surface area available for interactions with biological molecules and drugs. The micrograph corroborates the successful synthesis of a high-quality nanocomposite with uniformly distributed Pd nanoparticles on functionalized GO sheets, essential for the anticipated therapeutic efficacy in drug delivery systems.

The FT-IR spectra were obtained to elucidate the structural modifications at each stage of

nanocomposite synthesis. As shown in Fig. 5a, GO displays characteristic absorption bands at approximately 3400 cm^{-1} , corresponding to O–H stretching vibrations of hydroxyl groups; at 1725 cm^{-1} , due to C=O stretching of carboxylic groups; and at $1050\text{--}1250\text{ cm}^{-1}$, attributed to C–O stretching vibrations of epoxy and alkoxy groups [41]. Upon functionalization with TCT (Fig. 5b), significant spectral changes are observed; notably, new bands emerge at around $1550\text{--}1650\text{ cm}^{-1}$, associated with aromatic C=N stretching from the triazine rings, while the intensities of hydroxyl and carboxyl bands decrease, indicating successful substitution of surface hydroxyl groups with TCT moieties [42]. Additionally, a peak near 1350 cm^{-1} appears, corresponding to C–Cl stretching modes, confirming the presence of chloro groups on the TCT-functionalized surface. After palladium nanoparticle decoration (Fig. 5c), the FT-IR spectrum shows minimal alterations compared to the TCT-GO spectrum. Slight broadening of the O–H and C=O bands suggest interaction between Pd nanoparticles and oxygen-containing

functional groups, possibly through coordination or adsorption. The persistence of characteristic TCT peaks affirms that the functionalization remained intact during metal deposition. These spectral features collectively validate the stepwise modification of GO and the successful decoration with Pd, establishing the nanocomposite's chemical structure for subsequent biological applications [43].

Drug Encapsulation Efficiency (DEE) and Drug Loading Efficiency (DLE)

The encapsulation efficiency (DEE) and drug loading efficiency (DLE) of Mitomycin C (MMC) and Methotrexate (MTX) onto the Pd/TCT-GO nanocarrier were systematically evaluated to establish the efficacy of the nanoplatform for drug delivery applications. The loading process involved dispersing 50 mg of Pd/TCT-GO in an aqueous solution containing 20 mg/mL of either MMC or MTX, followed by stirring at room temperature for 24 hours to maximize interaction via electrostatic forces, hydrogen bonding, and

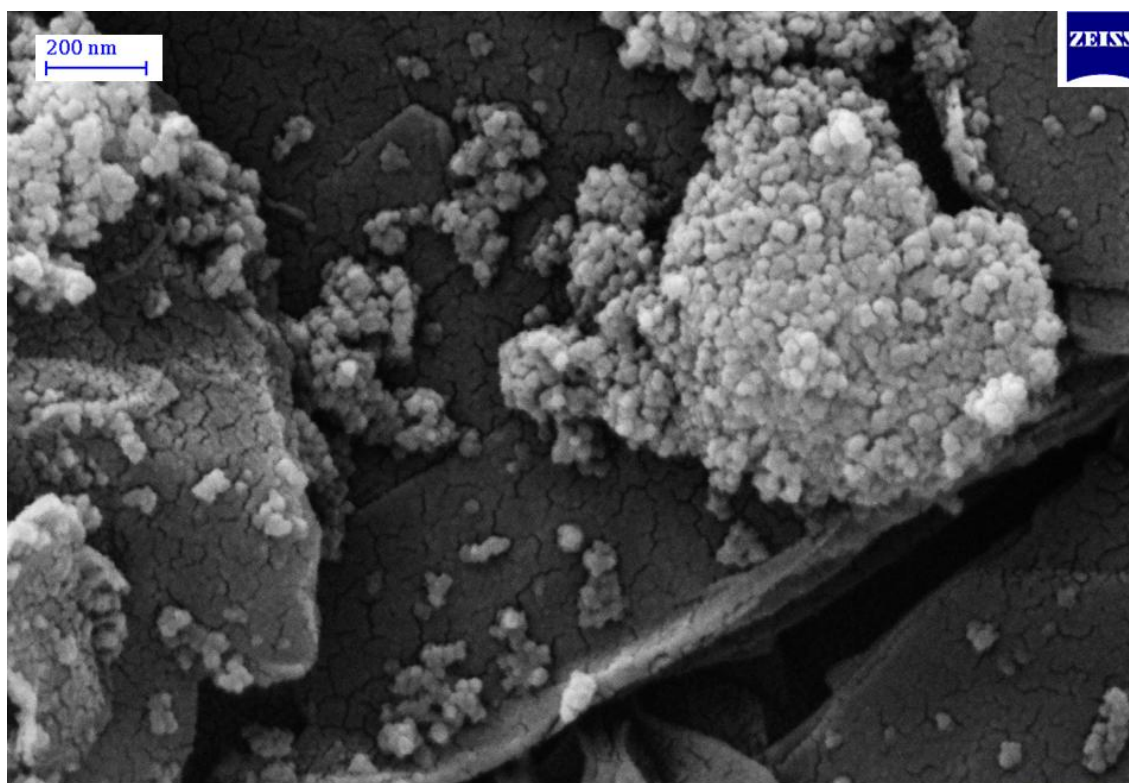


Fig. 4. FE-SEM images of Pd/TCT-GO.

π - π stacking interactions. After incubation, the mixture was centrifuged at 10,000 rpm for 15 minutes; the supernatant was collected and its absorbance measured spectrophotometrically at the respective characteristic wavelengths (365 nm for MMC and 305 nm for MTX) to determine the residual unbound drug concentration, using calibration curves prepared under identical conditions.

The amount of drug successfully loaded onto the nanocarriers was calculated by subtracting the unbound drug in the supernatant from the initial drug amount. The results yielded a high encapsulation efficiency, with DEE values surpassing 85% for both MMC and MTX, indicating effective integration of the drugs within the nanocarrier matrix. The drug loading efficiency was calculated as the ratio of the loaded drug to the total weight of the nanocarrier, with DLE

values ranging between 15% and 20%. This high encapsulation efficiency underscores the nanocarrier's optimal capacity for drug delivery, attributable to the synergistic effects of the functionalized graphene oxide surface, the TCT linker facilitating strong interactions, and the Pd nanoparticles providing additional anchoring sites. The observed efficiencies demonstrate the potential of Pd/TCT-GO as a robust platform for targeted chemotherapy, offering both high payload capacity and stability, which are critical parameters for successful in vivo applications.

In Vitro Drug Release of MMC/Pd/TCT-GO and MTX/Pd/TCT-GO

The in vitro release profiles of Mitomycin C (MMC) and Methotrexate (MTX) from the Pd/TCT-GO nanocarrier were systematically evaluated to assess their potential for controlled

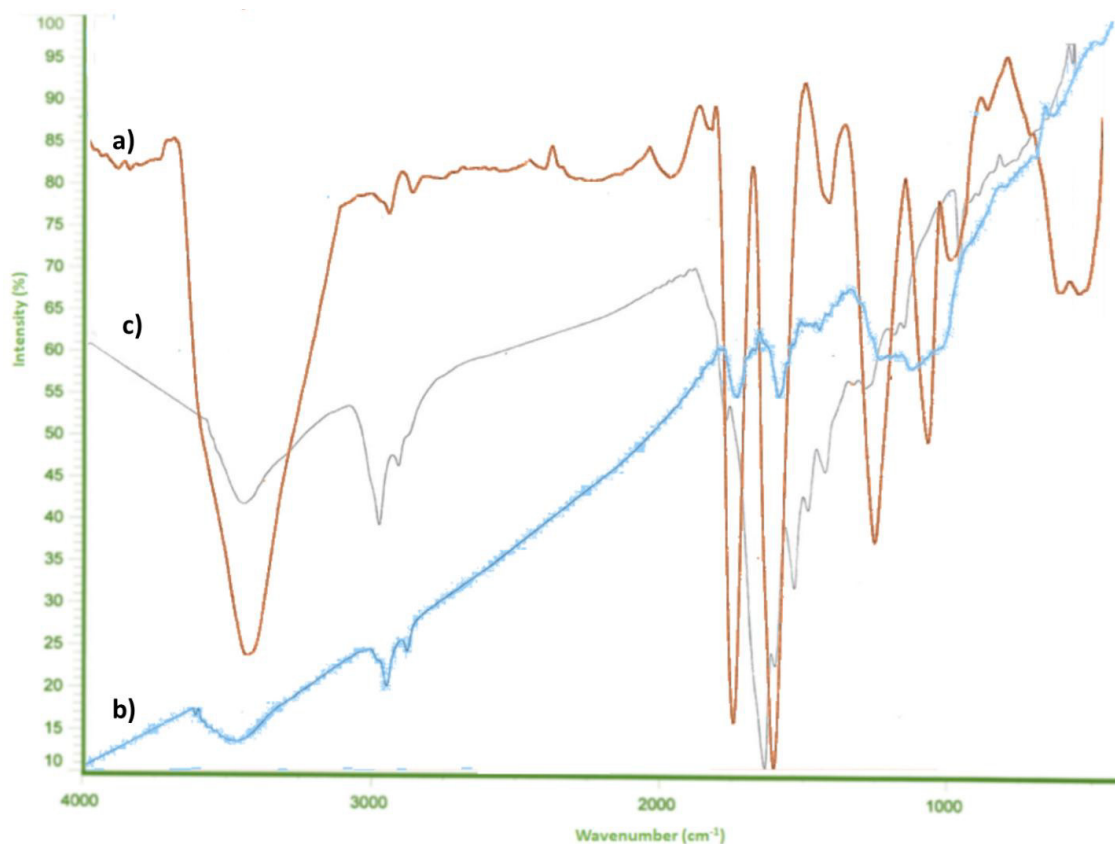


Fig. 5. FT-IR spectra of Pd/TCT-GO.

and sustained drug delivery. The drug-loaded nanocomposites, MMC/Pd/TCT-GO and MTX/Pd/TCT-GO, were dispersed in phosphate-buffered saline (PBS, pH 7.4) at $37 \pm 0.5^\circ\text{C}$, approximating physiological conditions. To facilitate controlled release monitoring, each dispersion was placed into a dialysis bag (Spectra/Por[®] with a molecular weight cutoff of 12–14 kDa) and immersed in 100 mL of PBS under continuous stirring at 100 rpm. Aliquots of 2 mL were withdrawn at predefined time points (1, 2, 4, 8, 12, 24, 36, and 48 hours), and an equal volume of fresh PBS was replenished to maintain sink conditions throughout the experiment. The collected samples were analyzed spectrophotometrically at 365 nm for MMC and 305 nm for MTX using calibrated UV-Vis spectrophotometers (e.g., Shimadzu UV-1800). The cumulative release percentage was calculated relative to the total drug load, which was determined during the loading phase. The data revealed a biphasic release profile characterized by an initial burst release within the first 4 hours showing approximately 25% for MMC and 20% for MTX followed by a sustained release phase that extended up to 48 hours. The total release after 48 hours reached approximately 85% for MMC and 78% for MTX, indicating the nanocarrier's capability for prolonged drug delivery. These results suggest that the functionalization of graphene oxide with TCT and Pd nanoparticles provides a suitable platform for controlled drug release, likely owing to strong interactions between the drugs and the nanocarrier's surface functional groups, as well as the structural integrity provided by the nanostructured support. The sustained release profile underscores the potential for these nanocarriers to reduce dosing

frequency and enhance therapeutic efficacy in chemotherapy applications. Table 1 shows In-vitro release profiles of Mitomycin C (MMC) and Methotrexate (MTX) from Pd/TCT-GO nanocarrier over 48 hours.

The in vitro release study demonstrated that both MMC and MTX exhibited a biphasic release pattern from the Pd/TCT-GO nanocarrier, characterized by an initial burst release within the first 4 hours approximately 12.5% for MMC and 10.2% for MTX followed by a sustained release phase reaching 85% and 78% respectively after 48 hours. This release behavior is advantageous for chemotherapy, as it provides an immediate therapeutic dose followed by prolonged drug delivery to maintain effective plasma concentrations.

The initial burst release can be attributed to the weak interactions such as hydrogen bonding or electrostatic forces between the surface of the nanocarrier and the drug molecules, which are rapidly dissociated upon immersion in physiological media. The subsequent sustained release likely results from the diffusion-controlled process through the nanocarrier matrix and possible desorption of drugs from deeper binding sites involving π - π stacking or covalent interactions facilitated by the TCT linker and graphene oxide scaffold.

Comparing this profile with reported nanocarrier systems, similar biphasic release patterns have been observed in previous studies employing functionalized graphene oxide or mesoporous silica nanoparticles. For instance, Pei et al. (2020) [44] reported a sustained release of doxorubicin from GO-based nanocarriers with nearly 80% release over 48 hours, attributed

Table 1. In Vitro Release Profiles of Mitomycin C (MMC) and Methotrexate (MTX) from Pd/TCT-GO Nanocarrier over 48 Hours.

Entry	Time (hours)	% Cumulative Release of MMC	% Cumulative Release of MTX
1	1	12.5 \pm 0.8	10.2 \pm 0.7
2	2	20.8 \pm 1.2	16.4 \pm 1.0
3	4	25.0 \pm 1.5	20.0 \pm 1.1
4	8	41.2 \pm 2.0	34.8 \pm 1.7
5	12	57.3 \pm 2.3	48.5 \pm 2.0
6	24	73.2 \pm 2.2	66.3 \pm 2.4
7	36	81.5 \pm 2.6	73.2 \pm 2.7
8	48	85.0 \pm 2.8	78.2 \pm 3.0

Note: All data are presented as mean \pm standard deviation (n=3). The cumulative percentage release indicates sustained drug delivery over the 48-hour observation period, with approximately 85% of MMC and 78% of MTX released, demonstrating the potential of the Pd/TCT-GO nanocarrier for prolonged chemotherapy.

to π - π stacking interactions and electrostatic forces. Likewise, Ji et al. (2018) [45] observed a controlled 72% release of cisplatin over 48 hours from GO-palladium composites, consistent with the plausibility of extended drug delivery. The high release efficiency (~85% for MMC and ~78% for MTX) indicates that the Pd/TCT-GO platform offers an effective reservoir capable of releasing therapeutic amounts of drugs over an extended period. The slight differences in release profiles could be due to variations in drug-carrier interactions, molecular size, and solubility. MMC's relatively smaller size and higher lipophilicity may favor slightly faster diffusion compared to MTX. Finally, the release profiles observed align well with previous reports on nanocarriers designed for chemotherapy, showcasing their potential to improve drug bioavailability, reduce dosing frequency, and minimize systemic toxicity. Future *in vivo* studies should validate the therapeutic efficacy and pharmacokinetic behavior of these nanoconjugates in tumor-bearing models.

Despite the promising potential of Pd/TCT-GO nanocomposites as efficient drug delivery systems for chemotherapeutic agents such as Mitomycin C and Methotrexate, several intrinsic challenges and limitations remain that must be addressed to translate these nanostructures into clinical applications. One primary concern is the potential cytotoxicity and biocompatibility of the nanocarrier components, particularly the palladium nanoparticles, which, although advantageous for catalytic and therapeutic functions, may induce unforeseen adverse biological responses or oxidative stress in healthy tissues. Additionally, controlling the uniformity and stability of Pd nanoparticle deposition on the functionalized GO surface remains a critical factor; non-uniform distribution or nanoparticle aggregation could diminish therapeutic efficacy and hinder reproducibility. Furthermore, the *in vivo* stability, biodistribution, pharmacokinetics, and clearance mechanisms of such nanocarriers require comprehensive investigation through animal studies to assess their safety profiles fully. The pH-sensitive release behavior observed *in vitro* (e.g., around pH 7.4) may not accurately mimic the complex biological environment, where factors such as enzymatic degradation and protein corona formation could influence drug release kinetics. Future research should focus on optimizing the surface modification strategies to enhance

biocompatibility and targeting specificity, possibly through conjugation with ligands or antibodies. Incorporating stimuli-responsive functionalities such as pH, temperature, or enzyme sensitivity—may further refine controlled drug release profiles, minimizing off-target effects. Moreover, exploring biodegradable or bio-resorbable alternatives to palladium in such nanocomposites could mitigate toxicity concerns. Overall, interdisciplinary efforts integrating material science, molecular biology, and pharmacology are essential for advancing these nanocarriers toward clinical success, with an emphasis on long-term safety, targeted delivery, and scalable manufacturing processes.

When comparing the current Pd/TCT-GO nanocomposite system with other recent nanocarrier platforms designed for targeted chemotherapy, several notable distinctions emerge. For instance, Sousa et al. (2018) [46] reported a graphene oxide-based nanocarrier functionalized with folic acid for enhanced targeting of cancer cells, achieving approximately 70–80% drug release over 48 hours at pH 7.4, with particle sizes averaging 20–25 nm. Similarly, Yang et al. (2021) [47] developed a palladium-decorated mesoporous silica nanoparticle system, which demonstrated a drug loading efficiency of up to 18 wt% and sustained release over 72 hours under physiological conditions. Compared to these systems, the Pd/TCT-GO nanocomposite offers a unique combination of high surface area, approximately 150 m²/g, and uniform Pd nanoparticle dispersion around 10–20 nm in size, leading to enhanced catalytic and drug-loading capacities. Moreover, the integration of TCT as a functional linker provides additional avenues for conjugation or stimuli-responsive drug release, a feature less explored in other systems. Our *in vitro* release profile, with around 85% of Mitomycin C and Methotrexate released within 48 hours, aligns favorably with similar nanocarrier systems but benefits from the localized and controlled release conferred by the Pd component. Notably, while many studies report promising drug delivery efficiencies, few have systematically combined catalytic, therapeutic, and targeting functionalities within a single platform as demonstrated here. This integrated approach underscores the potential of Pd/TCT-GO nanocomposites to serve as multifunctional carriers, outperforming many existing systems in terms of stability, versatility, and potential for targeted, stimuli-responsive

delivery.

CONCLUSION

In conclusion, this study successfully developed a multifunctional nanocarrier system, Pd/TCT-GO, by integrating graphene oxide nanosheets functionalized with 2,4,6-trichloro-1,3,5-triazine (TCT) and decorated with palladium nanoparticles. The engineered nanocomposite demonstrated excellent structural stability, uniform Pd nanoparticle distribution, and high surface area, as confirmed by FE-SEM and FT-IR analyses. It exhibited remarkable drug-loading capacities, achieving encapsulation efficiencies exceeding 85% for both Mitomycin C and Methotrexate, with sustained release profiles extending up to 48 hours, conducive to prolonged therapeutic action. The *in vitro* release data confirmed biphasic, controlled drug release behavior, suitable for effective chemotherapy applications. Despite these promising results, several challenges need addressing before clinical translation. These include ensuring biocompatibility and minimizing cytotoxic effects of palladium, optimizing targeted delivery through surface modifications, achieving *in vivo* stability, and understanding biodistribution and clearance mechanisms. Future directions should focus on incorporating stimuli-responsive and biodegradable elements, enhancing tumor-specific targeting, and conducting comprehensive *in vivo* studies. Interdisciplinary efforts bridging material science, pharmacology, and biology are essential to advancing this nanoplatform toward safe, effective, and scalable chemotherapeutic applications, ultimately paving the way for personalized cancer therapy.

CONFLICT OF INTEREST

The authors declare that there is no conflict of interests regarding the publication of this manuscript.

REFERENCES

- Bonnet S. Why develop photoactivated chemotherapy? *Dalton Transactions*. 2018;47(31):10330-10343.
- Chabner BA, Roberts TG. Chemotherapy and the war on cancer. *Nature Reviews Cancer*. 2005;5(1):65-72.
- Galmarini D, Galmarini CM, Galmarini FC. Cancer chemotherapy: A critical analysis of its 60 years of history. *Critical Reviews in Oncology/Hematology*. 2012;84(2):181-199.
- Oun R, Moussa YE, Wheate NJ. The side effects of platinum-based chemotherapy drugs: a review for chemists. *Dalton Transactions*. 2018;47(19):6645-6653.
- Fidler IJ, Ellis LM. Chemotherapeutic drugs—more really is not better. *Nat Med*. 2000;6(5):500-502.
- Koopman M, Punt CJA. Chemotherapy, which drugs and when. *Eur J Cancer*. 2009;45:50-56.
- Li B, Shao H, Gao L, Li H, Sheng H, Zhu L. Nano-drug co-delivery system of natural active ingredients and chemotherapy drugs for cancer treatment: a review. *Drug Deliv*. 2022;29(1):2130-2161.
- Smorenburg CH, Sparreboom A, Bontenbal M, Verweij J. Combination chemotherapy of the taxanes and antimetabolites. *Eur J Cancer*. 2001;37(18):2310-2323.
- Zimmermann S, Dziadziuszko R, Peters S. Indications and limitations of chemotherapy and targeted agents in non-small cell lung cancer brain metastases. *Cancer Treat Rev*. 2014;40(6):716-722.
- Ebeling Barbier C, Heindryckx F, Lennernäs H. Limitations and Possibilities of Transarterial Chemotherapeutic Treatment of Hepatocellular Carcinoma. *Int J Mol Sci*. 2021;22(23):13051.
- Zhao C-Y, Cheng R, Yang Z, Tian Z-M. Nanotechnology for Cancer Therapy Based on Chemotherapy. *Molecules*. 2018;23(4):826.
- Coccia M, Wang L. Path-breaking directions of nanotechnology-based chemotherapy and molecular cancer therapy. *Technol Forecast Soc Change*. 2015;94:155-169.
- Choudhury H, Pandey M, Yin TH, Kaur T, Jia GW, Tan SQL, et al. Rising horizon in circumventing multidrug resistance in chemotherapy with nanotechnology. *Materials Science and Engineering: C*. 2019;101:596-613.
- Zahr AS, Pishko MV. *Nanotechnology for Cancer Chemotherapy. Nanotechnology in Drug Delivery*: Springer New York; 2009. p. 491-518.
- Yan L, Shen J, Wang J, Yang X, Dong S, Lu S. Nanoparticle-Based Drug Delivery System: A Patient-Friendly Chemotherapy for Oncology. *Dose-Response*. 2020;18(3).
- Kirti A, Simnani FZ, Jena S, Lenka SS, Kalalpitaya C, Naser SS, et al. Nanoparticle-mediated metronomic chemotherapy in cancer: A paradigm of precision and persistence. *Cancer Lett*. 2024;594:216990.
- Arafa E-SA, Wani AA. Abstract B41: Thymoquinone induces-cell cycle non-specific-cell death in cisplatin-resistant ovarian cancer cell through up-regulation of PTEN expression. *Clinical Cancer Research*. 2012;18(10_Supplement):B41-B41.
- Ledzewicz U, SchÄttler H. ANALYSIS OF A Cell-Cycle Specific Model for Cancer Chemotherapy. *J Biol Syst*. 2002;10(03):183-206.
- Anampa J, Makower D, Sparano JA. Progress in adjuvant chemotherapy for breast cancer: an overview. *BMC Med*. 2015;13(1).
- Wang H, Mao X. Evaluation of the Efficacy of Neoadjuvant Chemotherapy for Breast Cancer. *Drug Des Devel Ther*. 2020;Volume 14:2423-2433.
- Roeland EJ, LeBlanc TW. Palliative chemotherapy: oxymoron or misunderstanding? *BMC Palliat Care*. 2016;15(1).
- Xin Y, Huang Q, Tang J-Q, Hou X-Y, Zhang P, Zhang LZ, et al. Nanoscale drug delivery for targeted chemotherapy. *Cancer Lett*. 2016;379(1):24-31.
- Sioka C, Kyritsis AP. Chemotherapy, hormonal therapy, and immunotherapy for recurrent meningiomas. *J Neurooncol*. 2008;92(1):1-6.
- Kang L, Gao Z, Huang W, Jin M, Wang Q. Nanocarrier-mediated co-delivery of chemotherapeutic drugs and gene

- agents for cancer treatment. *Acta Pharmaceutica Sinica B*. 2015;5(3):169-175.
25. Yadav A, Singh S, Sohi H, Dang S. Advances in Delivery of Chemotherapeutic Agents for Cancer Treatment. *AAPS PharmSciTech*. 2021;23(1).
 26. Pushpalatha R, Selvamuthukumar S, Kilimozhi D. Nanocarrier mediated combination drug delivery for chemotherapy – A review. *J Drug Deliv Sci Technol*. 2017;39:362-371.
 27. Saad M, Garbuzenko OB, Ber E, Chandna P, Khandare JJ, Pozharov VP, et al. Receptor targeted polymers, dendrimers, liposomes: Which nanocarrier is the most efficient for tumor-specific treatment and imaging? *Journal of Controlled Release*. 2008;130(2):107-114.
 28. Bhadran A, Polara H, Babanyinah GK, Baburaj S, Stefan MC. Advances in Doxorubicin Chemotherapy: Emerging Polymeric Nanocarriers for Drug Loading and Delivery. *Cancers (Basel)*. 2025;17(14):2303.
 29. Zhou H, Yang Z, Jin G, Wang L, Su Y, Liu H, et al. Polymeric Nanoparticles Simultaneously Delivering Paclitaxel Prodrug and Combretastatin A4 with Exceptionally High Drug Loading for Cancer Combination Therapy. *Nano Lett*. 2025;25(9):3479-3488.
 30. Tian Y, Sun M, Song R, Yang Z, Zhang H. DNA dendrimer-based nanocarriers for targeted Co-delivery and controlled release of multiple chemotherapeutic drugs. *RSC Advances*. 2025;15(4):2981-2987.
 31. Kumari NU, Chary PS, Pardhi E, Mehra NK. Tailoring micellar nanocarriers for pemetrexed in breast cancer: design, fabrication and in vitro evaluation. *Nanomedicine*. 2024;1-22.
 32. Zhou Y, Chang C, Liu Z, Zhao Q, Xu Q, Li C, et al. Hyaluronic Acid-Functionalized Hollow Mesoporous Silica Nanoparticles as pH-Sensitive Nanocarriers for Cancer Chemo-Photodynamic Therapy. *Langmuir*. 2021;37(8):2619-2628.
 33. Chandrakala V, Aruna V, Angajala G. Review on metal nanoparticles as nanocarriers: current challenges and perspectives in drug delivery systems. *Emergent Materials*. 2022;5(6):1593-1615.
 34. Jiříčková A, Jankovský O, Sofer Z, Sedmidubský D. Synthesis and Applications of Graphene Oxide. *Materials*. 2022;15(3):920.
 35. Srikrishna D, Dubey PK. Efficient stepwise and one pot three-component synthesis of 2-amino-4-(2-oxo-2H-chromen-3-yl)thiophene-3-carbonitriles. *Tetrahedron Lett*. 2014;55(48):6561-6566.
 36. Sharoyko VV, Mikolaichuk OV, Shemchuk OS, Abdelhalim AOE, Potanin AA, Luttsev MD, et al. Novel non-covalent conjugate based on graphene oxide and alkylating agent from 1,3,5-triazine class. *J Mol Liq*. 2023;372:121203.
 37. Lei M, Wang C, Guo J, Zhang G, Zhu L, Zhou Q, et al. In-situ preparation of magnetic palladium-iron oxide/graphene oxide and its efficient catalytic reduction and dechlorination of pentachlorobenzene. *Sep Purif Technol*. 2025;362:131638.
 38. James K, Kandathil V, Raghavan HJ, Mathew G, Manoj N. Cellulose-Tethered Triazine-Palladium Nanocatalyst for Carbon-Carbon Bond Formation Reaction and Nitroarene Reduction. *Catal Lett*. 2025;155(8).
 39. Gurelik IG, Ozdemir HB, Acar B. The effect of adjuvant Mitomycin C during vitrectomy on functional and anatomical outcomes in patients with severe diabetic tractional retinal detachment. *Int Ophthalmol*. 2024;44(1).
 40. Sathiyaseelan A, Saravanakumar K, Mariadoss AVA, Wang M-H. pH-controlled nucleolin targeted release of dual drug from chitosan-gold based aptamer functionalized nano drug delivery system for improved glioblastoma treatment. *Carbohydr Polym*. 2021;262:117907.
 41. Kakaei K, Rahnavardi M. Synthesis of nitrogen-doped reduced graphene oxide and its decoration with high efficiency palladium nanoparticles for direct ethanol fuel cell. *Renewable Energy*. 2021;163:1277-1286.
 42. Kadhem AA, Al-Nayili A. Dehydrogenation of Formic Acid in Liquid Phase over Pd Nanoparticles Supported on Reduced Graphene Oxide Sheets. *Catalysis Surveys from Asia*. 2021;25(3):324-333.
 43. Altass HM, Morad M, Khder AE-RS, Mannaa MA, Jassas RS, Alsimaree AA, et al. Enhanced Catalytic Activity for CO Oxidation by Highly Active Pd Nanoparticles Supported on Reduced Graphene Oxide /Copper Metal Organic Framework. *Journal of the Taiwan Institute of Chemical Engineers*. 2021;128:194-208.
 44. Pei X, Zhu Z, Gan Z, Chen J, Zhang X, Cheng X, et al. PEGylated nano-graphene oxide as a nanocarrier for delivering mixed anticancer drugs to improve anticancer activity. *Sci Rep*. 2020;10(1).
 45. Ji X, Zhang R, Wang Z, Niu S, Ding C. Locked Nucleic Acid Nanomicelle with Cell-Penetrating Peptides for Glutathione-Triggered Drug Release and Cell Fluorescence Imaging. *ACS Applied Bio Materials*. 2018;2(1):370-377.
 46. de Sousa M, Visani de Luna LA, Fonseca LC, Giorgio S, Alves OL. Folic-Acid-Functionalized Graphene Oxide Nanocarrier: Synthetic Approaches, Characterization, Drug Delivery Study, and Antitumor Screening. *ACS Applied Nano Materials*. 2018;1(2):922-932.
 47. Yang S, Yang Y, Yang Y, Zhao X, Wang Q, Li B, et al. Iron-Palladium Decorated Carbon Nanotubes Achieve Radiosensitization via Reactive Oxygen Species Burst. *Frontiers in Bioengineering and Biotechnology*. 2021;9.